forests

MDPI

Article

Triterpenoids Biosynthesis Regulation for Leaf Coloring of Wheel Wingnut (*Cyclocarya paliurus*)

Caowen Sun [1,2], Shengzuo Fang [1,2] and Xulan Shang [1,2,*]

[1] College of Forestry, Nanjing Forestry University, Nanjing 210037, China; scw19871217@126.com (C.S.); fangsz@njfu.edu.cn (S.F.)
[2] Co-Innovation Center for Sustainable Forestry in Southern China, Nanjing Forestry University, Nanjing 210037, China
* Correspondence: shangxulan@njfu.edu.cn

Abstract: *Cyclocarya paliurus* leaves are rich in triterpenoids with positive results in the treatment of diabetes, antioxidation, and scavenging free radicals. *C. paliurus* red leaves have been found to contain higher flavonoids including anthocyanin, however, the triterpenoids accumulation pattern is still unclear. For the purpose of researching the triterpenoid accumulating mechanism during red new leaf development, transcriptome and metabolome analysis was conducted during *C. paliurus* the red leaf development process. The results uncovered that most triterpenoid ingredients were found to accumulate during leaves turning green, while the unique ingredients content including cyclocaric acid A, cyclocarioside I, cyclocarioside II and cyclocarioside III decreased or remained unchanged. Functional structure genes (hydroxymethylglutaryl-CoA synthase, hydroxymethylglutaryl-CoA reductase, and farnesyl-diphosphate synthase) were identified for promoting triterpenoids accumulation mainly in the mevalonic acid pathway (MVA). Moreover, glycosyltransferase (UGT73C, UGT85A, and UGT85K) was also found attributed to triterpenoids accumulation. These findings provide information for a better understanding of the triterpenoid biosynthesis mechanism during leaf development and will be useful for targeted breeding.

Keywords: *Cyclocarya paliurus*; triterpenoids; differentially expressed genes; leaf coloration; secondary metabolites

Citation: Sun, C.; Fang, S.; Shang, X. Triterpenoids Biosynthesis Regulation for Leaf Coloring of Wheel Wingnut (*Cyclocarya paliurus*). *Forests* **2021**, *12*, 1733. https://doi.org/10.3390/f12121733

Academic Editor: Om P. Rajora

Received: 11 November 2021
Accepted: 6 December 2021
Published: 9 December 2021

1. Introduction

Cyclocarya paliurus (Batalin) Iljinsk. is a tree species only distributed in subtropical areas of China, and the tree leaves contain abundant health benefits such as secondary metabolite [1–3]. Among them, triterpenoids and flavonoids have been found to exhibit strong bioactivities. Health-benefitting triterpenoids including cyclocarioside I, cyclocarioside II, cyclocarioside III, cyclocaric acid A, and cyclocaric acid B are unique ingredients contained in *C. paliurus* leaves [4]. Furthermore, high levels of oleanolic acid and arjunolic acid also improved the bioactivities of total triterpenoids. In previous research, *C. paliurus* triterpenoids have shown positive results in the treatment of diabetes, antioxidation, scavenging free radicals, and improving drinking flavor [5,6].

Recently, *C. paliurus* germplasm with red new leaves—with high content of total flavonoids and triterpenoids—was selected for targeted breeding [7]. It was found that the red new leaves in plants always accumulate more flavonoids (anthocyanins) [7,8], while the triterpenoids accumulation pattern has not been previously studied in *C. paliurus* resources with red new leaves. The synthesis pathway of plant triterpenes is mainly the mevalonic acid pathway (MVA) and mevalonate pathway (MEP) [9], while flavonoids biosynthesis is mainly through the phenylpropane pathway [10]. According to a previous study, triterpenoids and flavonoids exhibited accumulating differences between different *C. paliurus* genotypes [6]. Therefore, comprehensive and systematic studies are needed for analyzing the total triterpenoids and triterpenoid variation pattern in leave coloring stages.

Transcriptomic and metabolomic methods have helped progress the analysis of plant tissue metabolites dynamics [11–13]. Screening and selection of plant evaluation are directly dependent on differences in chemical composition, metabonomics method (which has unique advantages in the evaluation of medicinal plants for testing multiple ingredients at the same time) [14], comprehensive testing data [13], directly fitting the metabolic pathway, and conducting association analysis with transcriptomic results [12]. In this research, for the purpose of studying triterpenoids dynamics during *C. paliurus* leaf coloring, transcriptomic and metabolomic methods were conducted in different leaf color development stages. Information regarding the triterpenoids biosynthesis mechanism and related genetic basis will help make progress on *C. paliurus* targeted breeding processes, and provide evidence on the accumulation pattern of target triterpenoids related to leaf quality and bioactivity.

2. Materials and Methods

2.1. Plant Materials

The plant samples were red leaves clones of *C. paliurus* LC1 (the *C. paliurus* clone). The leaf samples were collected from 3-year-old clones of LC1 from *C. paliurus* germplasm garden located in Nanjing City, Jiangsu Province, China. Different leaf development stages were separated according to the leaf color as shown in Figure 1 (red young leaf stage, half red leaf stage, and old green leaf stage), then sampled, transferred to dry ice, and stored in a −80 °C refrigerator for further transcriptomic and metabolomic analysis. Three biological replicates were designed for each leaf sample (total of 9 samples) and leaf samples for transcriptomic and metabolomic analysis were collected, respectively.

Figure 1. The leave phenotypes of the LC1 (the *C. paliurus* clone) during different growing periods. (**A**) LC1 leaves in old green leaf period; (**B**) LC1 leaves in semi-red leaf period; (**C**) LC1 leaves in young red leaf period; (**D**) LC1 clones.

2.2. Determination of Triterpenoids

The triterpenoids of leaf samples were detected by the UPLC-ESI-MS/MS system (UPLC, SHIMADZU Nexera X2, Kioto, Japan, www.shimadzu.com.cn/, accessed on 10 April 2021; MS, Applied Biosystems 4500 Q TRAP, (Applied Biosystems, Framingham, MA, USA, www.appliedbiosystems.com.cn/, accessed on 10 April 2021) at Wuhan MetWare Biotechnology Co., Ltd. (www.metware.cn/, accessed on 10 April 2021). The analytical conditions were as according to Yuan et al. (2018) and Zhang et al. (2020) [15,16].

The freeze-dried sample was crushed using a mixer mill (MM 400, Retsch, Haan, Germany) with a zirconia bead for 1.5 min at 30 Hz. One hundred milligrams of powder was weighted and extracted overnight at 4 °C with 1.2 mL 70% aqueous methanol. Following centrifugation at 12,000 rpm for 10 min, the extracts were filtrated (SCAA-104, 0.22μm pore

size; ANPEL, Shanghai, China, http://www.anpel.com.cn/, accessed on 10 April 2021) before UPLC-MS/MS analysis [15,16].

The analytical conditions were as follows: UPLC: column, Agilent SB-C18 (1.8 µm, 2.1 mm × 100 mm, Agilent Technologies, Santa Clara, CA, USA); The mobile phase consisted of solvent A, pure water with 0.1% formic acid, and solvent B, acetonitrile with 0.1% formic acid. Sample measurements were performed with a gradient program that employed the starting conditions: 95% A, 5% B. Within 9 min, a linear gradient to 5% A, 95% B was programmed, and a composition of 5% A, 95% B was kept for 1 min. Subsequently, a composition of 95% A, 5.0% B was adjusted within 1.10 min and kept for 2.9 min. The column oven was set to 40 °C; the injection volume was 4 µL. The effluent was alternatively connected to an ESI-triple quadrupole-linear ion trap (QTRAP)-MS [15,16].

LIT and triple quadrupole (QQQ) scans were acquired on a triple quadrupole-linear ion trap mass spectrometer (Q TRAP), AB4500 Q TRAP UPLC/MS/MS system, equipped with an ESI Turbo ion-spray interface, operating in positive and negative ion mode and controlled by Analyst 1.6.3 software (AB Sciex, Framingham, MA, USA). The ESI source operation parameters were as follows: ion source, turbo spray; source temperature, 550 °C; ion spray voltage (IS), 5500 V (positive ion mode)/−4500 V (negative ion mode); ion source, gas I (GSI), gas II (GSII), curtain gas (CUR) set at 50, 60, and 25.0 psi, respectively; the collision gas (CAD) was high. Instrument tuning and mass calibration were performed with 10 and 100 µmol/L polypropylene glycol solutions in QQQ and LIT modes, respectively. QQQ scans were acquired as MRM experiments with collision gas (nitrogen) set to medium. DP and CE for individual MRM transitions were carried out with further DP and CE optimization. A specific set of MRM transitions were monitored for each period according to the metabolites eluted within this period.

The principal component analysis of data was performed in R (www.r-project.org, accessed on 17 April 2021). The data were log-transformed (log2) and mean centered before OPLS-DA analysis. VIP values were extracted from OPLS-DA results using the R package MetaboAnalystR. Identified secondary metabolites were annotated using the KEGG Compound database (http://www.kegg.jp/kegg/compound/, accessed on 17 April 2021) and mapped to the KEGG pathway database (http://www.kegg.jp/kegg/pathway.html/, accessed on 17 April 2021).

2.3. RNA Extraction, Quantification and Sequencing

Leaf samples (3 samples with 3 replicates, respectively) were constructed for transcriptome sequencing on the Illumina Hiseq 2500 platform (Illumina Inc., San Diego, CA, USA). Referencing Sheng et al. (2021) [10], leaf samples RNA extraction, quantification, and transcriptome sequencing were performed and 150 bp paired-end reads were generated. The raw data of RNA were submitted at: www.ncbi.nlm.nih.gov/bioproject/PRJNA723183, accessed on 17 April 2021.

2.4. Transcriptome Data Analysis

The transcriptome data analysis was conducted according to Qiao et al. (2019). Low-quality sequences of raw data were filtered out by FastQC (http://www.bioinformatics.babraham.ac.uk/projects/fastqc/, accessed on 20 April 2021). The clean reads were then assembled by Trinity (Version r20140717) [17] by the paired-end method [18]. Unigenes were constructed and annotated by BLAST software [19] referencing the databases: Kyoto Encyclopedia of Genes and Genomes (KEGG), Gene Ontology (GO), Clusters of Orthologous Groups (COG), euKaryotic Orthologous Groups, Swissprot, NR, and Pfam [20]. The sequenced clean reads were compared with the UniGene library using Bowtie [21] and estimated by RSEM [22]. The FPKM (fragments per kilobase of exon per million fragments mapped) was calculated to evaluate gene expression level by featureCounts v1.5.0-p3 [23]. Differentially expressed genes (DEGs) were determined as >2 fold change and false discovery rate (FDR) correction set at $p < 0.05$ using the DESeq2 R package.

3. Results

3.1. Triterpenoid Individuals Analysis

According to Table 1, 42 triterpenoid individuals were identified from constructed leaf samples. To the total triterpenoids, the relative content (ion abundance) increased from the red new leaf stage (2.87×10^7 in A stage) to the old green leaf stage (9.7×10^7 in C stage). According to the Log2FC value, individuals with higher levels including madasiatic acid, 3-O-(2-O-Acetyl-glucosyl) oleanolic acid, and pomolic acid increased from C stage to A stage with log2FC C vs. A being 2.1, 1.0, and 3.3; while most unique ingredients in *C. paliurus* leaves decreased in the leaf development process, including cyclocarioside I (log2FC CvsA being −1.8), cyclocariosid III (log2FC BvsA being −1), and cyclocaric acid A (log2FC CvsA being −1). Furthermore, cyclocariosid II showed no statistical difference during each leaf development stage. On the other hand, triterpenoids with stronger bioactivity including 2-hydroxyoleanolic acid and arjunic acid also increased from the red new leaf stage to the old green leaf stage, with log2FC CvsA being 3.8 and 3.5.

Table 1. Differentially accumulated triterpenoids during the growing process of LC1 leaves.

Compounds	A (Ion Abundance)	B (Ion Abundance)	C (Ion Abundance)	CvsB	BvsA	CvsA
Madasiatic acid	3.64×10^7	1.86×10^7	8.59×10^6	1.1	1.0	2.1
3-O-(2-O-acetyl-glucosyl)oleanolic acid	1.60×10^7	1.27×10^7	8.06×10^6			1.0
2α-hydroxyursolic acid	4.95×10^6	2.53×10^6	1.63×10^6		1.0	1.6
11-keto-ursolic acid	1.46×10^6	1.84×10^6	1.58×10^6			
α-amyrenone	1.21×10^6	1.52×10^6	1.55×10^6			
Pomolic acid	1.34×10^7	4.91×10^6	1.38×10^6	1.8	1.5	3.3
Betulin	1.05×10^6	1.06×10^6	1.17×10^6			
Cyclocarioside III	4.77×10^5	9.55×10^5	8.04×10^5		−1.0	
3,24-dihydroxy-17,21-semiacetal-12(13) oleanolic fruit	3.35×10^6	8.01×10^5	5.10×10^5		2.1	2.7
3β,19α-dihydroxyolean-12-en-28-oic acid	3.73×10^5	3.83×10^5	4.64×10^5	1.8		
Alphitolic acid	4.72×10^6	1.20×10^6	3.37×10^5	1.9	2.0	3.8
Maslinic acid	4.70×10^6	1.25×10^6	3.36×10^5	1.8	1.9	3.8
2-hydroxyoleanolic acid	4.50×10^6	1.10×10^6	3.25×10^5	−1.0	2.0	3.8
Betulinic acid	3.79×10^4	7.14×10^4	1.47×10^5			−2.0
Lupenone	3.51×10^4	4.78×10^4	1.27×10^5			−1.9
p-coumaroyleuscaphic acid	7.96×10^4	1.24×10^5	1.24×10^5			
Cyclocarioside I	2.21×10^4	6.08×10^4	7.51×10^4	1.5	−1.5	−1.8
Cyclocaric acid A	3.67×10^4	6.32×10^4	7.12×10^4			−1.0
Madecassic acid	9.26×10^4	1.06×10^5	6.74×10^4	−1.4		
Camaldulenic acid	2.01×10^5	1.11×10^5	4.05×10^4	1.7		2.3
Taraxerol	4.55×10^4	4.32×10^4	2.87×10^4			
Ursolic acid	2.18×10^5	1.07×10^5	2.74×10^4		1.0	3.0
Rosamultic acid	1.86×10^4	9.82×10^3	2.57×10^4			
24,30-dihydroxy-12(13)-enolupinol	1.93×10^5	8.47×10^4	2.56×10^4	2.6	1.2	2.9
3β-[(arabinosyl)oxy]-28-norurs-12,17-dien	1.88×10^4	2.13×10^4	2.45×10^4			
3β-hydroxy-28-norurs-17,19,21-trien	2.09×10^4	2.61×10^4	1.91×10^4			
oleanolic acid-3-O-glucosyl(1→2)glucoside	1.16×10^4	1.46×10^4	1.90×10^4			
3,11-dioxo-19α-hydroxyurs-12-en-28-oic acid	2.81×10^4	1.70×10^4	1.80×10^4			
oleanolic acid-3-O-glucuronide	1.29×10^4	1.80×10^4	1.14×10^4			
Terminolic acid	3.15×10^5	5.13×10^4	8.71×10^3		2.6	5.2
Arjunic acid	7.44×10^4	9.31×10^3	6.67×10^3		3.0	3.5
Cyclocarioside II	4.01×10^3	6.27×10^3	5.99×10^3			
Tormentic acid	2.90×10^4	9.49×10^3	5.50×10^3		1.6	2.4
Rutundic acid	3.29×10^4	8.37×10^3	4.60×10^3		2.0	2.8

(**A**) LC1 leaves in green leave period; (**B**) LC1 leaves in semi-red leave period; (**C**) LC1 leaves in young red leave period. (CvsB) = Log2 fold change between C and B stage; (BvsA) = Log2 fold change between B and A stage; (CvsA) = Log2 fold change between C and A stage.

3.2. RNA-seq and Data Analysis

The differentially expressed genes (DEGs) were analyzed by the transcriptome method. Nine leaf samples in total yielded 64.36 Gb clean data with 93% of bases scoring Q30, and 26,4908 unique genes were expressed. According to the principal component analysis (PCA) of FPKM values, nine samples (3 samples with 3 biological replicates) were clearly separated into three growing stages, respectively, exhibiting accuracy and reliability of our experiment data (Figure 2A). DEGs from A, B, and C stages were screened, annotated, and clustered (Figure 2). According to KEGG enrichment (Figure 2E), it was found that the metabolites and secondary metabolites biosynthesis-related genes occupied most DEGs. Among secondary metabolites biosynthesis, DEGs were found in sesquiterpenoids and triterpenoids biosynthesis along with flavonoids biosynthesis and isoflavonoids biosynthesis. In total, 852 DEGs (Figure 2D) overlapping expression in CvsA, CvsB, and BvsA was screened, meaning they might be key DEGs regulated in the leaf development stage. Among these conservative genes, triterpenoids biosynthesis-related unigenes were found including 1-deoxy-D-xylulose-5-phosphate synthase (Cluster-7239.2898, Cluster-7239.130383), alpha-farnesene synthase (Cluster-7239.77779), (3S,6E)-nerolidol synthase (Cluster-3255.0), (-)-germacrene D synthase (Cluster-7239.155003, Cluster-7239.161173), and lupeol synthase (Cluster-7239.65073, Cluster-7239.59075, Cluster-7239.80579, Cluster-7239.144814, Cluster-7239.77098). All DEGs were then clustered by the K-means method and separated into six clusters according to expression differences during three leaf development stages (Figure 2C). Among them, 5528 unigenes in sub-class 6 exhibited gradient high expression levels in the old green leaf stage, moderate levels in the half red leaf stage, and low levels in the red new leaf stage. Unigenes regulating triterpenoid biosynthesis were also found in sub-class 6 including hydroxymethylglutaryl-CoA reductase, farnesyl diphosphate synthase, farnesyl-diphosphate farnesyltransferase, diphosphomevalonate decarboxylase, hydroxymethylglutaryl-CoA synthase, isopentenyl-diphosphate Delta-isomerase, isopentenyl phosphate kinase, alpha-farnesene synthase, (3S,6E)-nerolidol synthase, (-)-germacrene D synthase, beta-amyrin synthase, NAD +-dependent farnesol dehydrogenase, and lupeol synthase. On the contrary, 2794 unigenes in sub-class 2 exhibited down-regulation during the C to A leaf development stage, also containing triterpenoid biosynthesis-related unigenes: hydroxymethylglutaryl-CoA reductase (NADPH), squalene monooxygenase, 1-deoxy-D-xylulose-5-phosphate synthase, and 1-deoxy-D-xylulose-5-phosphate synthase. In sub-class 3, 2299 unigenes exhibited a random variation trend, meaning they might not be correlated with triterpenoid accumulation.

UDP-glucosyltransferase is also considered a regulated factor in triterpenoid biosynthesis [11–13]. According to our analysis, related UGT unigenes were also identified including UDP-glucosyltransferase 73C (5 unigenes), UDP-glucosyltransferase 75B1 (2 unigenes), UDP-glucosyltransferase 73B2 (2 unigenes), cyanohydrin UDP-glucosyltransferase-UGT85K (3 unigenes), and UDP-glucosyltransferase 85A (1 unigenes). Notably, UGT73B2 (Cluster-7239.138070, Cluster-7239.150441), UGT85K (Cluster-7239.198214, Cluster-7239.80990), and UGT85A (Cluster-7239.41467) were clustered into sub-class 6 according to the K-means method, meaning they are highly correlated with triterpenoid accumulation; while UDP-glucosyltransferase 75B1 unigenes (Cluster-7239.124835, Cluster-7239.26044) were clustered into sub-class 2, implying a negative regulation. Despite being clustered into sub-class 5, UDP-glycosyltransferase 73C3 unigenes (Cluster-7239.140635, Cluster-7239.50887, Cluster-7239.106623, Cluster-7239.90121) still showed significantly higher expression in the A stage than C stage, showing positive effects as UGT73B2, UGT85K, and UGT85A [14]. In addition, P450 family genes have also been considered triterpenoid synthesis regulators in previous studies. Although the P450 family DEGs were identified by KEGG annotation including CYP73A (1 unigene), CYP4B1(5 unigenes), CYP734A1 (6 unigenes), CYP82G1 (3 unigenes), CYP736A (15 unigenes), and CYP77A (1 unigene), they were not directly correlated with triterpenoid biosynthesis in previous studies [14]. Even so, CYP736A (14 unigenes) and CYP734A1 (6 unigenes) showed significant up-regulation in the A stage compared to the C stage.

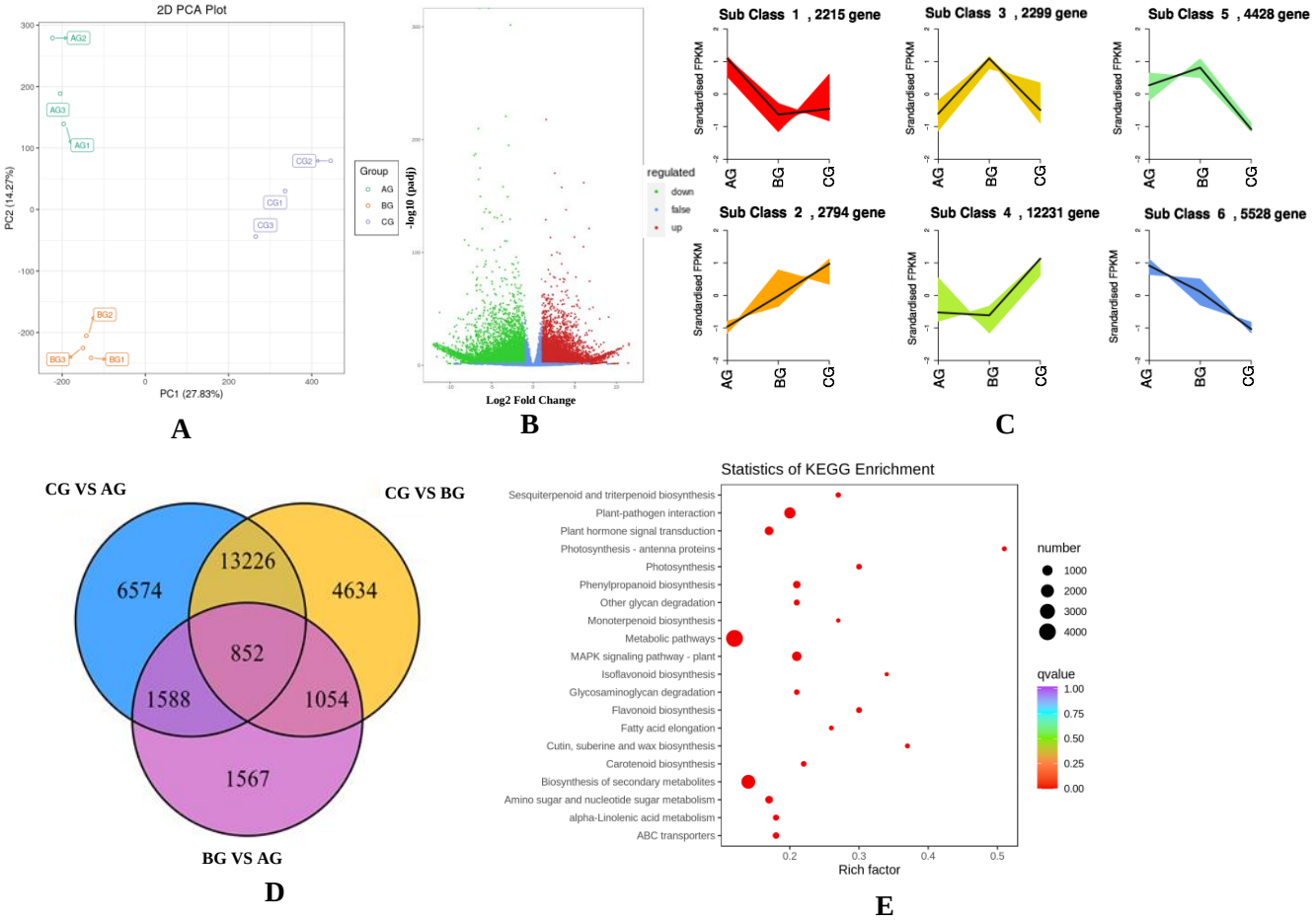

Figure 2. Differential expressed genes (DEG) in growing leaves of LC1. (**A**) PCA plots displaying DEG of LC1 leaves in A, B and C stage with 3 replicates, (**B**) Volcano plots displaying the up-regulated, down-regulated, and no-regulated genes between green-colored and red-colored leave samples, (**C**) Venn diagram showing the shared and unique DEGs between the 3 compared groups of leave samples. AG = genes expression in old green leave period; BG = gene expression in semi-red leave period; CG = gene expression in new red leave period; (**D**) DEGs clusters according to the expression level in different leave coloring period. (**E**) Top KEGG terms contributed by DEGs of CG vs. AG.

3.3. Transcriptomic and Metabolomic Association Analysis

According to the transcriptome and metabolome analysis, we constructed the triterpenoid biosynthesis pathway to uncover the mechanism regulating triterpenoids accumulation during leaf development of LC1 [11–13]. In Figure 3, structure genes showed significant expression differences; most detected structure genes showed a random regulating trend except HMGS (hydroxymethylglutaryl-CoA synthase), HMGR (hydroxymethylglutaryl-CoA reductase), and FPPS (farnesyl-diphosphate synthase). HMGS and HMGR belong to the MVA pathway of terpenoids biosynthesis pathway, promoting the transformation from acetyl CoA to MVA. On the contrary, the MEP pathway was not active compared to the MVA pathway and DXS (1-deoxy-D-xylulose-5-phosphate synthase) was relatively silent during leaf development. In addition to the triterpenoids backbones biosynthesis pathway, FPPS (farnesyl-diphosphate synthase) exhibited an active expression level while other structure genes were relatively silent including GPPS (geranyl-diphosphate synthase) and SM (squalene monooxygenase). In the lupane-type triterpenoid saponins biosynthesis pathway, LS (lupeol synthase) DEGs were detected with a relatively random expression level. Metabolome analysis results showed that total triterpenoids increased during leaf growth, and most triterpenoids including madasiatic acid and 3-O-(2-O-Acetyl-glucosyl) oleanolic acid exhibited significant increases. It could be inferred that up-regulation of the MVA pathway promoted an increase in total triterpenoids.

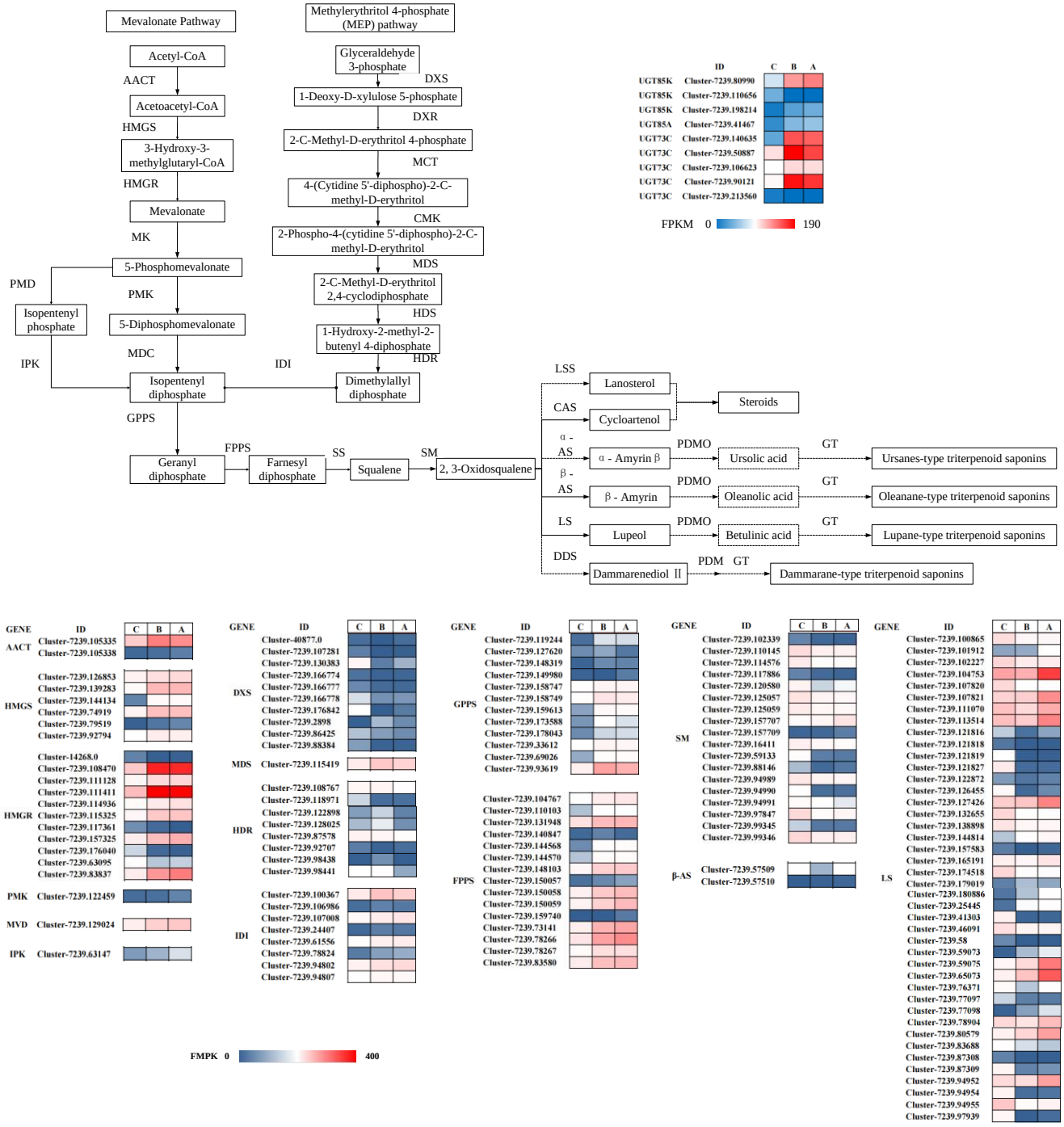

Figure 3. Modulation of triterpenoids biosynthesis pathway genes during growing process of LC1 leaves. The histogram displays the expression levels of the genes (FPKM value). The charts in blue and red represent the down and upregulated structural genes. AACT: acetyl-CoA C-acetyltransferase, HMGR: hydroxymethylglutaryl-CoA reductase, HMGS: hydroxymethylglutaryl-CoA synthase, PMD: phosphomevalonate decarboxylase, IPK: isopentenyl phosphate kinase, MK: mevalonate kinase, PMK: phosphomevalonate kinase, MDC: diphosphomevalonate decarboxylase, GPPS: geranyl-diphosphate synthase, DXR: 1-deoxy-D-xylulose-5-phosphate reductoisomerase, DXS: 1-deoxy-D-xylulose-5-phosphate synthase, MCT: 2-C-methyl-D-erythritol 4-phosphate cytidylyltransferase, MDS: 2-C-methyl-D-erythritol 2,4-cyclodiphosphate synthase, CMK: 4-diphosphocytidyl-2-C-methyl-D-erythritol kinase, MCT: 2-C-methyl-D-erythritol 4-phosphate cytidylyltransferase. HDR: 4-hydroxy-3-methylbut-2-en-1-yl diphosphate reductase, HDS: (E)-4-hydroxy-3-methylbut-2-enyl-diphosphate synthase, IDI: isopentenyl-diphosphate Delta-isomerase, IPP: Isopentenyl pyrophosphate, GPPS: geranyl-diphosphate synthase, FPPS: farnesyl-diphosphate synthase, SM: squalene monooxygenase, SS: squalene synthase, LS: lupeol synthase, LSS: lanosterol synthase, CAS: cycloartenol synthase, α-AS: α-amyrin synthase, β-AS: β-amyrin synthase, DDS: dammarenediol II synthase.

According to previous research, CYP450 s and glycosyltransferase (UGTs) have been considered to be involved in the biosynthesis of triterpene saponins [9]. CYP450 s catalyzes the structural modification of the triterpene backbones for hydroxylation, carboxylation, alkylation, kekylation, and dehydrodehydration to form the intermediate of triterpene saponins. Triterpene glycosylation catalyzed by UGTs is often considered the last step in triterpene saponin biosynthesis, leading to the diversity of triterpene saponin and bioactivity formation. In this study, 32 DEGs of CYP450 s and 14 DEGs of UGTs were screened during different leaf development periods. Among them, 26 CYP450 s and 10 DEGs were up-regulated in the old green leaf period. At the same time, 5 UGT73C, 1 UGT85A, and 3 UGT85K exhibited significant expression differences during LC1 leaf development mainly from the UGT73 and 85 families. These UGTs families were tightly correlated to triterpene saponins biosynthesis, and 4 UGT73C, 1 UGT85A, and 2 UGT85K were up-regulated in the old green leaf period.

4. Discussion

Triterpenoids participate in plant communication, defense, and sensory control, and also have biological activities such as anti-inflammatory, anti-cancer, anti-bacterial, and antiviral [9]. *C. paliurus* triterpenoid was found to be antidiabetic by promoting glucose uptake and improving lipid metabolism [24–26]. Furthermore, cyclocaric acid A, cyclocaric acid B, and cyclocarioside I, II, and III were ingredients particularly in *C. paliurus*, and cyclocarioside I sweetness is about 200 times that of sucrose [4]. Other triterpenoids including oleanolic acid and ursolic acid were also found to show anti-cancer bioactivity in animal and cell experiments [27]. *C. paliurus* triterpenoid has been studied in previous research, including pentacyclic triterpenoid and secodammarane triterpenoid. Among them, ursanes-type, oleanane-type, and lupane-type belong to pentacyclic triterpenoid. Oleanane-type triterpenoid saponins have been identified in *C. paliurus* leaves including oleanolic acid, arjunic acid, cyclocaric acid A and B; ursanes-type triterpenoid saponins have been identified including 2α-Hydroxyursolic acid, 11-keto-ursolic acid, and asiatic acid; lupane-type triterpenoid saponins have been identified including betulinic acid [28]. At the same time, more dammarane-type triterpenoid saponins have been identified in recent years including cyclocarioside I, II, and III, and other dammarane-type triterpenoid saponins with unique structures that were uncovered gradually, including cyclocarioside O, cyclocarioside P, and cyclocarioside O-Q [29,30].

In this study, the triterpenoids in LC1 leaf samples from different growing periods were measured by HPLC-MS. Madasiatic acid, pomolic acid, 2α-hydroxyursolic acid (ursanes-type triterpenoid), and 3-O-(2-O-acetyl-glucosyl) oleanolic acid (oleanane-type triterpenoid) almost kept increasing during LC1 leaf development from red to green. Qin et al. (2020) [31] considered that nitrogen forms alter total triterpenoid and triterpenoid accumulation simultaneously. It could be inferred that LC1 leaf development may lead to tissue nitrogen content variation leading to changes in the corresponding triterpenoids.

Research related to *C. paliurus* transcriptome and metabolome profiling is relatively limited. Qin et al. (2020) [31] extracted RNA and used quantitative real-time polymerase chain reaction (qRT-PCR) analysis to study the triterpenoids accumulation in *C. paliurus* clones, finding that HMGR, DXR, GPS, SQS, β-AS, and UDP were influenced by nitrogen forms and the trend was general. Sun et al. (2020) [6] also found that the triterpenoid individuals of *C. paliurus* germplasm exhibited the same geographical variation characteristics as total triterpenoids. In this study, the results are in agreement with Qin et al. (2020) [31] and Sun et al. (2020) [6] that the triterpenoid individuals nearly kept the same variation pattern, implying that the main gene regulation occurred upstream of the biosynthesis pathways. HMGS, HMGR, and FPPS showed significance during LC1 leaf development, and HMGS and HMGR belong to the MVA pathway, certificating our hypothesis.

Chen et al. (2021) cloned CpHMGR, CpDXR, and CpSQS genes and tried to uncover the gene expression patterns, finding that CpSQS exhibited higher gene expression in leaves than shoot from July to October while CpHMGR and CpDXR were expressed oppositely [5].

Partly in agreement with Chen et al. (2021) [5], the downstream pathway genes FPPS in this study were found to play an important role in triterpenoid accumulation, while the upstream genes HMGS and HMGR in the MVA pathway also exhibited high expression. Other research on triterpenoids accumulation in different plant organs has been carried out including *Gleditsia sinensis* Lam., *Clinopodium chinense* (Benth.) Kuntze, and *Entada phaseoloides* (L.) Merr. [11–13], and the structure gene expression patterns between species were different. Our research found triterpenoids content in old green leaves than red new leaves, and this was associated with the MVA (HMGS and HMGR) pathway instead of the MEP pathway. Old green leaves with more photosynthates supplied more material basis for upstream triterpenoid biosynthesis, leading to a general increase in most triterpenoid individuals. On the other hand, arjunic acid, cyclocaric acid A, cyclocarioside I, II, and III showed random accumulation patterns, probably because of the much lower relative content.

In pentacyclic triterpene synthesis, skeleton glycosylation is the key modification reaction, which is achieved by glycosyltransferase [32]. Until now, glycosyltransferase involved in plant penticyclic triterpenoids modification mainly distributed in UGT71, 73, 74, 85, 91, and 94 families [9]. In this study, UGT73C, UGT85A, and UGT85K were identified in DEGs, and four out of five UGT73C unigenes exhibited significant high expression levels in old green leaves than red new leaves. Augustin et al. (2012) [32] considered that UGT73C10, UGT73C11, UGT73C12, and UGT73C13 could catalyze the glycosylation of hederin and oleanolic acid. In agreement with Augustin et al. (2012) [32], the old green leaves of LC1 generated more oleanane-type triterpenoid saponins including 3-O-(2-O-acetyl-glucosyl)oleanolic acid and 2-hydroxyoleanolic acid [33]. Cytochrome P450-dependent monooxygenase (CYP450 s, EC1.14.x.x) are key enzymes in the triterpene saponin biosynthesis pathway that catalyze the structural modification of hydroxylation, carboxylation, alkylation, ketone, and dehydrodehydration to form an intermediate of triterpene saponin [34]. CYP450 s—involved in the biosynthesis of plant triterpene saponins—comes mainly from the CYP51, CYP71, CYP72, and CYP85 families [9], however, our results did not identify DEGs related to these CYP families.

5. Conclusions

In this study, transcriptome and metabolome analysis was performed on three leaf samples in different growing periods of *C. paliurus*. Among 42 triterpenoid individuals, 15 triterpenoid individuals were found to accumulate at the old green leaf stage, while the most unique ingredients accumulated more at the red young leaf stage. The triterpenoids exhibited different variation patterns during leave color transformation. Key structural genes (HMGR, HMGS, and FPPS) were identified to play a role in the triterpenoid biosynthesis pathway. Moreover, UGT73C, UGT85A, and UGT85K were up-regulated in the old green leaf period. Our research uncovered the triterpenoid accumulation pattern and the mechanism of triterpenoids biosynthesis pathway during leaf development. The data set will help to better understand the triterpenoid biosynthesis mechanism during leaf development. This will help make progress in *C. paliurus* breeding with a high yield of triterpenoids.

Author Contributions: Methodology and experimental design, C.S.; data curation, C.S.; data analysis, C.S.; writing—original draft preparation, C.S.; writing—review and editing, S.F. and X.S.; funding acquisition, S.F. and X.S. All authors have read and agreed to the published version of the manuscript.

Funding: This work was supported by the Key Research and Development Program of Jiangsu Province (BE2019388), the National Natural Science Foundation of China (31971642, 32001305), the Priority Academic Program Development of Jiangsu Higher Education Institutions (PAPD) and the Doctorate Fellowship Foundation of Nanjing Forestry University. The funders had no role in study design, data collection and analysis, decision.

Acknowledgments: We would like to show gratitude to Fu Xiangxiang and Yang Wanxia for their assist in experiments.

Conflicts of Interest: The authors declare no conflict of interest.

References

1. Li, X.; Fu, X.; Shang, X.; Yang, W.; Fang, S. Natural population structure and genetic differentiation for heterodicogamous plant: *Cyclocarya paliurus* (Batal.) Iljinskaja (Juglandaceae). *Tree Genet. Genomes* **2017**, *13*, 80. [CrossRef]
2. Sun, C.; Zhou, Y.; Fang, S.; Shang, X. Ecological Gradient Analysis and Environmental Interpretation of *Cyclocarya paliurus* Communities. *Forests* **2021**, *12*, 146. [CrossRef]
3. Sun, C.; Zhong, W.; Fu, X.; Shang, X.; Fang, S. A study on growth and aboveground biomass production of juvenile *Cyclocarya paliurus* plantations. *J. Nanjing For. Univ. (Nat. Sci. Ed.)* **2021**, *10*, 387. Available online: https://kns.cnki.net/kcms/detail/32.1161.S.20210825.0918.002.html/ (accessed on 25 August 2021).
4. Fang, S.Z.; Fu, X.X. Progress and Prospects on Silviculture and Utilization of *Cyclocarya paliurus* Resources. *J. Nanjing For. Univ. (Nat. Sci. Ed.)* **2007**, *31*, 95–100.
5. Chen, X.; Chen, B.; Shang, X.; Fang, S. Rna in situ hybridization and expression of related genes regulating the accumulation of triterpenoids in *Cyclocarya paliurus*. *Tree Physiol.* **2021**, *41*, 2189–2197. [CrossRef] [PubMed]
6. Sun, C.; Shang, X.; Ding, H.; Cao, Y.; Fang, S. Natural Variations in Flavonoids and Triterpenoids of *Cyclocarya paliurus* Leaves. *J. For. Res.* **2020**, *31*, 805–814. [CrossRef]
7. Tian, L.; Xu, C.; Shang, X.; Fu, X. Evaluation and selection on superior individuals for medicinal use of *Cyclocarya paliurus*. *J. Nanjing For. Univ. (Nat. Sci. Ed.)* **2021**, *45*, 21–28. [CrossRef]
8. Han, M.; Yang, C.; Zhou, J.; Zhu, J.; Meng, J.; Shen, T.; Li, H. Analysis of flavonoids and anthocyanin biosynthesis-related genes expression reveals the mechanism of petal color fading of Malus hupehensis (Rosaceae). *Braz. J. Bot.* **2020**, *43*, 81–89. [CrossRef]
9. Xu, Y.; Chen, Z.; Jia, L.; Weng, X. Advances in understanding of the biosynthetic pathway and regulatory mechanism of triterpenoid saponins in plants. *Sci. Sin. Vitae* **2021**, *51*, 525–555. [CrossRef]
10. Sheng, X.; Chen, H.; Wang, J.; Zheng, Y.; Li, J. Joint transcriptomic and metabolic analysis of flavonoids in *Cyclocarya paliurus* leaves. *ACS Omega* **2021**, *6*, 9028–9038. [CrossRef] [PubMed]
11. Liao, W.; Mei, Z.; Miao, L.; Liu, P.; Gao, R. Comparative transcriptome analysis of root, stem, and leaf tissues of Entada phaseoloides reveals potential genes involved in triterpenoid saponin biosynthesis. *BMC Genom.* **2019**, *21*, 639. [CrossRef] [PubMed]
12. Shi, Y.Y.; Zhang, S.X.; Peng, D.Y.; Wang, C.K.; Zhao, D.R.; Ma, K.L.; Wu, J.W.; Huang, L.Q. Transcriptome Analysis of Clinopodium chinense (Benth.) O. Kuntze and Identification of Genes Involved in Triterpenoid Saponin Biosynthesis. *Int. J. Mol. Sci.* **2019**, *20*, 2643. [CrossRef] [PubMed]
13. Kuwahara, Y.; Nakajima, D.; Shinpo, S.; Nakamura, M.; Kawano, N.; Kawahara, N.; Yamazaki, M.; Saito, K.; Suzuki, H.; Hirakawa, H. Identification of potential genes involved in triterpenoid saponins biosynthesis in Gleditsia sinensis by transcriptome and metabolome analyses. *J. Nat. Med.* **2019**, *73*, 369–380. [CrossRef] [PubMed]
14. Xu, Y.; Gao, Y.; Chen, Z. Metabolomics analysis of the soapberry (Sapindus mukorossi Gaertn.) pericarp during fruit development and ripening based on UHPLC-HRMS. *Sci. Rep.* **2021**, *11*, 11657. [CrossRef]
15. Yuan, H.J.; Zeng, X.Q.; Shi, J.; Xu, Q.J.; Wang, Y.L.; Jabu, D.Z.; Sang, Z.; Nyima, T. Time-course comparative metabolite profiling under osmotic stress in tolerant and sensitive Tibetian hulless barley. *BioMed Res. Int.* **2018**, *9415409*, 1–12.
16. Zhang, Q.; Wang, L.; Liu, Z.; Zhao, Z.; Zhao, J.; Wang, Z.; Zhou, G.; Liu, P.; Liu, M. Transcriptome and metabolome profiling unveil the mechanisms of Ziziphus jujuba Mill. peel coloration. *Food Chem.* **2020**, *312*, 125903. [CrossRef]
17. Grabherr, M.G.; Haas, B.J.; Yassour, M.; Levin, J.Z.; Thompson, D.A.; Amit, I.; Adiconis, X.; Fan, L.; Raychowdhury, R.; Zeng, Q.; et al. Full length transcriptome assembly from RNA Seq data without a reference genome. *Nat. Biotechnol.* **2011**, *29*, 644–652. [CrossRef]
18. Yu, R.; Liang, X.; Wei, Z.; Wang, Y.; Luo, X.; Wang, R.; Zhu, X.; Xie, Y.; Karanja, B.; Liu, L. De novo taproot transcriptome sequencing and analysis of major genes involved in sucrose metabolism in Radish (Raphanus sativus L.). *Front. Plant Sci.* **2016**, *7*, 585. [CrossRef] [PubMed]
19. Altschul, S.F.; Madden, T.L.; Schäffer, A.A.; Zhang, J.; Zhang, Z.; Miller, W.; Lipman, D.J. Gapped BLAST and PSI BLAST: A New Generation of Protein Database Search Programs. *Nucleic Acids Res.* **1997**, *25*, 3389–3402. [CrossRef]
20. Qiao, Z.Q.; Liu, S.S.; Zeng, H.J.; Li, Y.X.; Wang, X.Y.; Chen, Y.; Wang, X.M.; Cai, N. Exploring the molecular mechanism underlying the stable purple-red leaf phenotype in lagerstroemia indica cv. ebony embers. *Int. J. Mol. Sci.* **2019**, *20*, 5636. [CrossRef]
21. Langmead, B.; Trapnell, C.; Pop, M.; Salzberg, S.L. Ultrafast and memory-efficient alignment of short DNA sequences to the human genome. *Genome Biol.* **2009**, *10*, R25. [CrossRef] [PubMed]
22. Li, B.; Colin, N.D. RSEM: Accurate transcript quantification from RNA Seq data with or without a reference genome. *BMC Bioinform.* **2011**, *12*, 323. [CrossRef]
23. Liao, Y.; Smyth, G.K.; Shi, W. featureCounts: An efficient general purpose program for assigning sequence reads to genomic features. *Bioinformatics* **2014**, *30*, 923–930. [CrossRef]
24. Wu, Z.; Gao, T.; Zhong, R.; Lin, Z.; Jiang, C.; Ouyang, S.; Zhao, M.; Che, C.; Zhang, J.; Yin, Z. Antihyperlipidaemic effect of triterpenic acid-enriched fraction from *Cyclocarya paliurus* leaves in hyperlipidaemic rats. *Pharm. Biol.* **2017**, *55*(1), 712–721. [CrossRef]
25. Fang, Z.J.; Shen, S.N.; Wang, J.M.; Wu, Y.J.; Zhou, C.X.; Mo, J.X.; Lin, L.G.; Gan, L.S. Triterpenoids from *Cyclocarya paliurus* that Enhance Glucose Uptake in 3T3-L1 Adipocyt. *Molecules* **2019**, *24*, 187. [CrossRef] [PubMed]

26. Zhu, K.N.; Jiang, C.H.; Tian, Y.S.; Xiao, N.; Wu, Z.F.; Ma, Y.L.; Lin, Z.; Fang, S.Z.; Shang, X.L.; Liu, K.; et al. Two triterpeniods from *Cyclocarya paliurus* (Batal) Iljinsk (Juglandaceae) promote glucose uptake in 3T3-L1 adipocytes: The relationship to AMPK activation. *Phytomedicine* **2015**, *22*, 837–846. [CrossRef] [PubMed]
27. Zhou, M.M.; Chen, P.; Shang, X.L.; Yang, W.X.; Fang, S.Z. Genotype-Environment Interactions for Tree Growth and Leaf Phytochemical Content of Cyclocarya paliurus (Batal.) Iljinskaja. *Forests* **2021**, *12*, 735. [CrossRef]
28. Tang, M.; Zhao, L.C.; Zhi, Y.H.; Zhang, Q.H. Chemical constituents and pharmacological activities of Cyclocarya paliurus (Batal.)Iljinskaja:research advances. *J. Int. Pharm. Res.* **2017**, *44*, 851–859.
29. Wang, Y.R.; Cui, B.S.; Han, S.W.; Li, S. New dammarane triterpenoid saponins from the leaves of *Cyclocarya paliurus*. *J. Asian Nat. Prod. Res.* **2018**, *20*, 1019–1027. [CrossRef]
30. Xuan, T.Y.; Tan, J.; Sun, H.H.; Yang, C.; Lv, W.Y.; Zhang, J.H.; Zhang, K.Q.; Nie, Z.Q.; Ye, Z.J.; He, X.A.; et al. Cyclocarioside O-Q, three novel seco-dammarane triterpenoid glycosides from the leaves of *Cyclocarya paliurus*. *Nat. Prod. Res.* **2021**, *35*, 167–173. [CrossRef] [PubMed]
31. Qin, J.; Yue, X.; Shang, X.; Fang, S. Nitrogen Forms Alter Triterpenoid Accumulation and Related Gene Expression in *Cyclocarya paliurus* (Batalin) Iljinsk. *Seedlings For.* **2020**, *11*, 631. [CrossRef]
32. Augustin, J.M.; Drok, S.; Shinoda, T.; Sanmiya, K.; Nielsen, J.K.; Khakimov, B.; Olsen, C.E.; Hansen, E.H.; Kuzina, V.; Ekstrom, C.T.; et al. UDP glycosyltransferases from the UGT73C subfamily in Barbarea vulgaris catalyze sapogenin 3-O-glucosylation in saponin-mediated insect resistance. *Plant Physiol* **2012**, *160*, 1881–1895. [CrossRef] [PubMed]
33. Rahimi, S.; Kim, J.; Mijakovic, I.; Jung, K.H.; Choi, G.; Kim, S.C.; Kim, Y.J. Triterpenoid-biosynthetic UDP-glycosyltransferases from plants. *Biotech. Adv.* **2019**, *37*, 107394. [CrossRef] [PubMed]
34. Thimmappa, R.; Geisler, K.; Louveau, T.; O'Maille, P.; Osbourn, A. Triterpene biosynthesis in plants. *Annu. Rev. Plant Biol.* **2014**, *65*, 225–257. [CrossRef] [PubMed]